Journal of Electron Spectroscopy and Related Phenomena 189 (2013) 157–163

Contents lists available at ScienceDirect

Journal of Electron Spectroscopy and Related Phenomena

journal homepage: www.elsevier.com/locate/elspec

# Surface magnons probed by spin-polarized electron energy loss spectroscopy

Kh. Zakeri*, Y. Zhang, J. Kirschner

*Max-Planck-Institut für Mikrostrukturphysik, Weinberg 2, D-06120 Halle, Germany*

ARTICLE INFO

*Article history:*
Available online 26 June 2012

*PACS:*
75.30.Ds
75.50.Bb
75.70.Ak

*Keywords:*
Spin-polarized electron energy-loss spectroscopy
Surface magnetism
Spin waves
Magnons
Magnetic excitations

ABSTRACT

Short-wavelength magnons at ferromagnetic surfaces can be probed by electrons. The unique property of electrons, i.e. having a very strong interaction with the surface together with the spin degree of freedom enables one to investigate the spin dependent quasi-particles, e.g. magnons at magnetic surfaces.

We review the experimental results of short-wavelength magnons probed at ferromagnetic Co(0 0 0 1) and Fe(1 1 0) surfaces by spin-polarized electron energy-loss spectroscopy. The differences and similarities to their bulk counterpart are discussed in detail. Although in the case of Co(0 0 0 1) surface magnons behave similar to the ones in bulk Co, in the case of Fe(1 1 0) they possess a smaller exchange stiffness meaning that the effective exchange coupling is smaller at the surface. In both cases, surface magnons have an extremely short lifetime being in the order of a few tens of femtosecond.



## 1. Introduction

Magnetism at surfaces and in ultrathin films has attracted a lot of attention because of exotic phenomena, which have not been observed in bulk materials [1–4]. Enhanced magnetic moment at the surface [3], perpendicular easy axis [4] and giant magnetoresistance effect [5,6] are all attributed to the presence of the surface and interface. The possibilities of using these new effects observed at the magnetic surfaces and interfaces in magneto-electronic technology have been extensively discussed and even some of the available devices in nowadays technology are based on these properties [7].

Magnetic excitations are well-established subjects in bulk magnetism. They are of crucial importance for understanding the microscopic origins of different observations in magnetism, e.g., the magnetic ordering phenomena at a finite temperature. From a fundamental physics point of view, a complete knowledge of magnetic excitations would lead to a better understanding of the physical phenomena related to the excited state of the system. In the case of low-dimensional magnetic objects or at surfaces, the magnetic excitations should, in principle, reflect the properties of these systems. This knowledge is essential to understand the theory of high-speed response of a magnetic material to different kinds of excitations (for instance high frequency electromagnetic radiations). Moreover, it would allow a prediction of the role and the type of elementary excitations generated within the processes like spin-current induced magnetic switching [8,9]. From the application point of view this information would help us to design magnetic devices, which can be operated at high frequencies.

In a classical description, the wavy-like motions of the atomic magnetic moments, which are caused by the precession of the individual moments are called spin waves. Their representative quasi-particles are referred to as magnons. Long-wavelength (low-energy) excitations are usually treated classically using phenomenological approaches, e.g., using the so-called Landau–Lifshitz–Gilbert (LLG) equation of motion. The dominating magnetic interaction for this class of magnons is the magnetic dipolar interaction [10,11]. Although in various occasions it is shown that the LLG equation fails to describe the magnetic damping mechanisms in ferromagnets [12–15], however, it lies in the central explanation of long-wavelength spin waves, at least where processes like two-magnon scattering are not important. In contrary to this class of magnons the short-wavelength magnons are governed by magnetic exchange interaction and therefore their properties are entirely different than those of long-wavelength magnons.

In this paper we will provide the experimental results of short-wavelength magnon excitations probed by spin-polarized electron energy-loss spectroscopy (SPEELS) on different ferromagnetic surfaces. As examples we discuss the results of Co(0 0 0 1) and Fe(1 1 0) films grown on W(1 1 0) surface. The results of magnon dispersion relation and the lifetime of surface magnons will be discussed.

* Corresponding author. Tel.: +49 345 5582749; fax: +49 345 5511223.
*E-mail address:* zakeri@mpi-halle.de (Kh. Zakeri).
*URL:* http://www.mpi-halle.de/ (Kh. Zakeri).

0368-2048/$ – see front matter © 2012 Elsevier B.V. All rights reserved.
http://dx.doi.org/10.1016/j.elspec.2012.06.009

Some comparison to the results of the bulk samples probed by inelastic neutron scattering (INS) measurements will be provided. The paper is organized as follows: In Section 2 we introduce the basic concepts needed to follow the paper. In Section 3, the experimental details concerning the sample preparation, characterization, and SPEELS measurements are provided. Section 4 is dedicated to the main experimental results followed by a discussion. A concluding remark is provided in Section 5.

## 2. Basic concepts

Spin waves governed by exchange interaction may be described by the classical Heisenberg Hamiltonian. In this description the representative quasi-particles of spin waves are referred to as magnons. The simplest form of Heisenberg spin Hamiltonian reads as:

$$H = -\sum_{i \neq j} J_{ij} \vec{S}_i \cdot \vec{S}_j. \tag{1}$$

Here $J_{ij}$ denotes the isotropic exchange interaction between spins $\vec{S}_i$ and $\vec{S}_j$. This Hamiltonian applies to a system of spins, which are coupled via an isotropic exchange interaction in the absence of any external magnetic field and magnetic anisotropy. In the systems with magnetic anisotropy, an additional term, which is proportional to the magnetic anisotropy energy of the system, should be added to Eq. (1). In the presence of the antisymmetric exchange interaction (usually referred to as Dzyaloshinskii–Moriya interaction [16,17]) an additional term, which is proportional to the vector product of the spins $(\vec{S}_i \times \vec{S}_j)$ may be added to the spin Hamiltonian [18].

In order to derive the equation of motion, in a semi-classical picture, one may consider the magnetic exchange interaction as the source of a torque acting on each magnetic moment. The equation of motion can be derived as:

$$\hbar \frac{d\vec{S}_i}{dt} = \vec{\tau}_i = 2\sum_j J_{ij} \left( \vec{S}_i \times \vec{S}_j \right). \tag{2}$$

Writing the expansion of the cross product in terms of spin components leads to the following equations:

$$\hbar \frac{dS_i^x}{dt} = 2\sum_j J_{ij} (S_i^y S_j^z - S_j^y S_i^z), \tag{3}$$

$$\hbar \frac{dS_i^y}{dt} = 2\sum_j J_{ij} (S_j^x S_i^z - S_i^x S_j^z). \tag{4}$$

Now if one defines the rising operator as $S^+ = S^x + iS^y$, Eq. (2) can be simplified to:

$$i\hbar \frac{dS_i^+}{dt} = 2S\sum_j J_{ij} \left[ S_i^+ - S_j^+ \right], \tag{5}$$

where $S \approx S^z$ denotes the magnitude of spin. By considering a wave form solution for the magnons ($S_i^+ = A_i \exp[i(\vec{q} \cdot \vec{R}_j - \omega t)]$, $A_i$ denotes the amplitude of the magnon with the wave vector $\vec{q}$ and angular frequency of $\omega$ at position $\vec{R}_i$) one can simply derive the following expression, which connects the magnons energy (eigenfrequency) to their wave vector:

$$\hbar\omega A_i = 2S \sum J_{ij} \{A_i - A_j \exp[i\vec{q} \cdot (\vec{R}_j - \vec{R}_i)]\}. \tag{6}$$

The above equation is usually used to derive the magnon dispersion relation for any system of interest. We will use it in Section 4 to calculate the dispersion relation of our systems. For an infinitely large crystal with simple cubic structure and considering only the nearest neighbor interaction, the dispersion relation can be written as this simple form:

$$E = \hbar\omega = 2zJS \left[ 1 - \frac{1}{z} \sum_\delta \cos(\vec{q} \cdot \vec{a}) \right], \tag{7}$$

where $z$ is the number of nearest neighbors, $J = J_{ij}$ represents the exchange coupling constant between the neighbors and $\vec{a}$ is the position vector of the respective neighbor. The Heisenberg Hamiltonian provides no information concerning the magnons' damping. The assumption is that the magnons live for an infinitely long time. In reality, the magnons possess a finite lifetime, which for the case of itinerant electron ferromagnets is quite short. We will provide some information on the magnon lifetimes at the Fe(1 1 0) surface in Section 4.2. The classical Heisenberg picture fails to describe the magnon dispersion relation in itinerant electron ferromagnets [19–31]. However, since it provides a simple way of understanding the magnon dispersion relation, we will use it for our data analysis in a comparative way.

In an itinerant ferromagnet the bands are spin-split across the Fermi-level, which can lead to a possibility of single-particle excitations called Stoner excitations. In fact, an electron of majority spin character can jump from an occupied majority band to an empty state in the minority band above the Fermi-level. A hole with majority spin character in the majority band will be left. The electron–hole pairs (Stoner pairs), generated within this process, possess a total spin of $1\hbar$. The energy and momentum of a Stoner pair is given by the momentum and energy difference of the electron and hole in the minority- and majority-band, respectively. The probability of having Stoner excitations depends on the band structure. In two-dimensional metallic ferromagnets, Stoner excitations are spread over the entire Brillouin zone and only a narrow area within the Stoner gap is left. They overlap with the collective excitations. It is shown that Stoner excitations lead to an energy renormalization of the high wave vector magnons, in addition to modifying their damping [28,29,32]. The excitations at very low energies (below the Stoner gap) will not be influenced by the Stoner continuum and may still be described in terms of spin waves.

## 3. Experimental details

For this study all the experiments were performed under ultra-high vacuum (UHV) condition with a base pressure better than $3 \times 10^{-11}$ mbar. As with other surface sensitive methods, performing SPEELS experiments in UHV is essential to get rid of the effects induced by adsorbates.

### 3.1. Sample preparation

The samples were grown in situ in the form of ultrathin films by the molecular beam epitaxy technique. The structure and chemical properties were characterized using low-energy electron diffraction (LEED) and Auger electron spectroscopy (AES). The magnetic properties were studied by magneto-optical Kerr effect (MOKE). The magnon excitations were investigated using SPEELS. In the following section we will briefly introduce our SPEELS spectrometer. We also discuss and describe the basic physical processes involved in SPEELS experiments.

### 3.2. Spin-polarized electron energy-loss spectroscopy

SPEELS is a spectroscopy technique based on the scattering of spin-polarized electrons from a magnetic surface. In this technique a spin-polarized low-energy electron beam is incident onto the sample surface at a certain scattering geometry and the intensity of the scattered electrons is measured versus their energy loss. As

it is a spin polarized version of electron energy-loss spectroscopy (EELS), some basic principles are similar to the one of EELS experiments. The main advantage of SPEELS is that one has a direct access to control the spin of the incoming beam and thereby can distinguish the spin dependent and spin independent excitations at solid surfaces. This is essential for investigating magnon excitations. No spin selective detection is involved in this experiment. The energy of the incoming beam has usually been chosen to be in the order of a few electron-volts (3–10 eV). This is the range, where the magnons are observed as pronounced peaks in the energy-loss spectra [33].

It is often thought that the basic concepts of SPEELS are similar to the one of the inelastic neutron scattering (INS). In fact the fundamental basis of these two techniques are different. In SPEELS experiments the exchange mechanism plays an important role while in INS experiments the type of the interaction that is important is the dipolar interaction between the neutron magnetic moment with the magnetic field induced by magnons. In the following we will discuss how does the exchange mechanism during the scattering process lead to magnon excitations within the SPEELS experiments.

Before we discuss the contributions to the inelastic scattering of the spin-polarized electrons, let us define the spin direction of the incoming and outgoing beam. It is defined with respect to the majority and minority spins of the sample. When the spin of the electron is parallel to the majority electrons of the ferromagnetic surface, it is called spin-up electron ↑ and when it is parallel to the minority electrons of the sample surface it is called spin-down electron ↓. Generally, the inelastic scattering of spin-polarized electrons is a rather complicated topic. A complete description of the mechanisms involved in such processes is out of the scope of the present paper. An extended discussion can be found in Ref. [34]. If an electron with a given spin (↑ or ↓) is incident onto a ferromagnetic surface at a certain geometry, the outgoing electron has either the spin orientation parallel or anti-parallel to the one of the incoming electron. Although in the former case an exchange of the electrons with the same spins is possible, in the latter case one can clearly talk about the exchange process. This means that the incident electron occupies an unoccupied state above the Fermi-level and another electron from an occupied state below the Fermi-level will be scattered out of the surface. The corresponding processes are schematically illustrated in Fig. 1 for incident of spin-down (left) and spin-up (right) electrons. The processes in which the incident and scattered electrons have the same spin character are usually referred to as "*non-flip*" processes and the ones in which the spin of the scattered electron is opposite to the incident electron are called "*flip*" processes. It is essential to notice that no direct spin reversal is involved in the processes mentioned above. The underlying mechanism is the exchange process. The "*flip*" process mentioned above describes the fact that an incident electron with given spin direction is exchanged with an electron from the sample with an opposite spin orientation (for an extended discussion see for example [34–38]).

As discussed in Section 2 the total angular momentum of a magnon is $1\hbar$. If a spin-down electron is incident onto the surface, it excites a majority electron from a state below the Fermi-level and occupies an empty state above the Fermi-level. The excited majority electron will be scattered out of the sample. Such a process leads to excitation of a magnon with a total angular momentum of $1\hbar$. A magnon annihilation process may be imagined when a spin-up electron is incident onto the sample surface. However, during this process the outgoing electron would gain energy and hence this process would take place in the energy gain spectra. As such a process requires an available magnon, the intensity of the peak associated with this process is proportional to the number of the available magnons. In the thermodynamic steady state condition the number of magnons is given by the Bose–Einstein statistics,

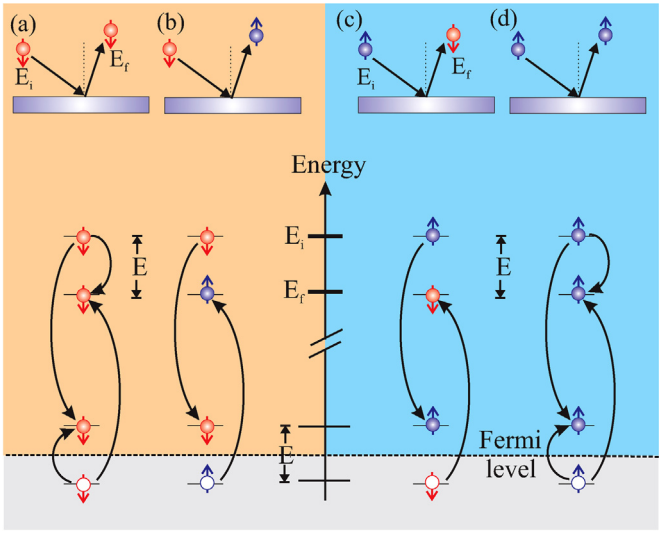


**Fig. 1.** A schematic representation of possible processes when a spin-down (a and b) or spin-up (c and d) electron is incident onto a magnetic surface. Since in processes shown as (a) and (d) the spin of the incident and scattered electron is the same we call these processes "*non-flip*" processes. Consequently processes (b) and (c) are called "*flip*" processes because the spin of the scattered electron is opposite to the one of the incident electron. Note that these processes are due to the exchange mechanism and no direct spin reversal process is involved here. The lower panel shows the corresponding excitation processes within the system. During such processes electrons from a state below the Fermi-level are excited and holes are created in the system. The incoming electron with energy $E_i$ transfers its energy to an electron in a state below the Fermi-level and fills an unoccupied state. The excited electron leaves the sample from a state with energy $E_f = E_i - E$.

since they are bosons. In the processes mentioned above when an electron is excited from a state below the Fermi-level a hole is left in the system. The resulting electron and hole in the system are correlated and are considered as an electron–hole pair. The energy and momentum of the corresponding electron–hole pair (magnon) is the energy and momentum difference of the electron and hole.

We note that during the scattering, phonons can also be excited at the surface. Since the phonons are spin independent quasiparticles they can be excited by incidence of spin-down as well as spin-up electrons. The answer to this question: "how one can distinguish between magnons and phonons when the phonons also show a spin asymmetry?" is out of the scope of this paper. In principle, comparing the gain and loss features of each excitation should provide an access to its nature. A detailed discussion may be found in Ref. [39].

Fig. 2 shows a schematic view of the scattering processes within the SPEELS experiments. Since the energy and the parallel momentum of the electrons are conserved during the scattering process, the wave vector of the magnons can be selected by adjusting the scattering geometry (see Fig. 2). This fact enables one to probe the magnons in a wave vector selective manner. Assuming that the energy and momentum before and after scattering are $E_i$, $\vec{k}_i$ and $E_f$, $\vec{k}_f$, respectively, the energy $E$ and the in-plane component of the wave vector $\vec{q}_\parallel$ of the excited magnons can be given by the following expressions:

$$\begin{aligned} E &= E_f - E_i \\ \left|\vec{q}_\parallel\right| &= \left|\Delta\vec{k}_\parallel\right| = \left|\vec{k}_i\right|\sin\theta - \left|\vec{k}_f\right|\sin(\theta_0 - \theta). \end{aligned} \tag{8}$$

Here, $\theta$ ($\theta_0$) is the angle between the incident beam and the surface normal (scattered beam).

The magnon dispersion relation can be obtained by performing the experiments at different wave vectors. The desired wave vector can be achieved by changing the angle between the incoming beam and the surface normal ($\theta$) or the angle between the incoming beam

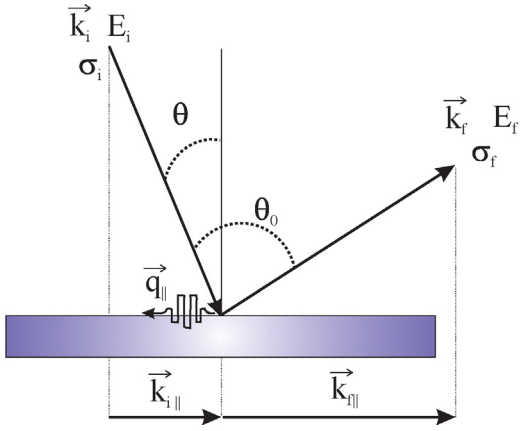


**Fig. 2.** A schematic representation of the scattering geometry in the SPEELS experiments. An electron beam with a given energy $E_i$, wave vector $\vec{k}_i$ and spin $\sigma_i$ is scattered from the surface to an electron beam with energy $E_f$, wave vector $\vec{k}_f$ and spin $\sigma_f$. Since the energy and the in-plane wave vector is conserved within this process, the energy and the wave vector of the excited magnons (the in-plane component) is given by Eq. (8).

and the outgoing one ($\theta_0$). In addition to the conservation of energy and parallel momentum, the total angular momentum has to also be conserved. Hence magnon excitations are allowed only when minority electrons are incident. This implies that the magnon peak will appear only in the minority spin channel. Magnon excitations are forbidden when majority electrons are incident onto the sample surface (see Fig. 3). We will come back to this point in Section 4.1.

## 4. Results and discussion

### 4.1. The magnon dispersion relation

Experimentally the properties of magnons like excitation energy (or eigenfrequency, $\omega = E/\hbar$, where $E$ is the excitation energy), dispersion relation and the lifetime are obtained by recording the energy-loss spectra. An example is given in Fig. 3, where typical SPEELS spectra measured on a hexagonal close-packed (hcp) Co(0 0 0 1) and a body-centered cubic (bcc) Fe(1 1 0) film recorded at a wave vector of 0.7 Å$^{-1}$ are presented. In the experiments one sequentially measures the spectra for both spin orientations of the incoming beam ($I_\uparrow$ and $I_\downarrow$). The peak in the minority spin channel ($I_\downarrow$) is due to the magnon excitations. The peak intensity is usually one or even two orders of magnitude smaller than the one of the elastic peak (the one at $E_{loss} = 0$). The small satellites in the upper panel of Fig. 3(b) at energies of about 63 and 120 meV are due to the vibrational excitations of the adsorbed oxygen and hydrogen from the residual gases in the chamber. Since they appear in both spin channels and show a very weak energy dispersion, they can be clearly identified. The magnon peak shows a finite width that provides information about the typical lifetime of the magnons. A way to analyze the magnon peaks is taking the difference spectra that is $I_\downarrow - I_\uparrow$ (see the lower panels of Fig. 3). We use the difference spectra for further data analysis.

For a thin film composed of a finite number of atomic layers, the Heisenberg model predicts $n$ different modes, where $n$ is the number of atomic layers. However, in the experiment irrespective of the number of atomic layers, only a single magnon peak was observed (the surface acoustic mode). The first reason may lie in the fact that in the case of the acoustic mode the moments precess in phase and hence the transverse components of spins are added to each other. Therefore this mode appears as a pronounced peak in the spectrum. The high-energy modes (the optical modes) are the results of the anti-phase precession of the spin moments. In such cases the transverse components of the spin moments may cancel out each other and hence no signal can be detected by SPEELS. The second reason might be the small excitation cross-section and the strong damping of the higher energy modes. The third reason might be due to the fact that the acoustic surface mode has the largest amplitude at the surface and the SPEELS technique is strongly surface sensitive.

In thin film systems monitoring the magnon excitation energy versus the film thickness would provide some information about the role of the surface structure and the interface effects on the magnons. Interestingly the measurements performed on ultrathin Co(0 0 0 1) films on W(1 1 0) showed that the excitation energy slightly increases when the thickness of the Co layer increases [40]. The same behavior was observed for Co(0 0 1) films on Cu(0 0 1) [41]. The measurements performed on Fe(1 1 0) films with different thicknesses on W(1 1 0) revealed that the excitation energy shows an unusual thickness dependence [42]. Fig. 4 shows the excitation energy at a given wave vector (0.5 Å$^{-1}$ or 0.7 Å$^{-1}$) versus the film thickness. The unusual thickness dependence of magnon energy could be understood in terms of lattice relaxation. Fe films grow pseudomorphically on W(1 1 0) from the initial stage of the growth up to a film thickness of about 2 monolayer (ML). As the third atomic layer is growing a network of dislocations start to form and the films start to relax towards the bulk structure [43–45]. This fact was confirmed by analysis of the LEED patterns recorded on the

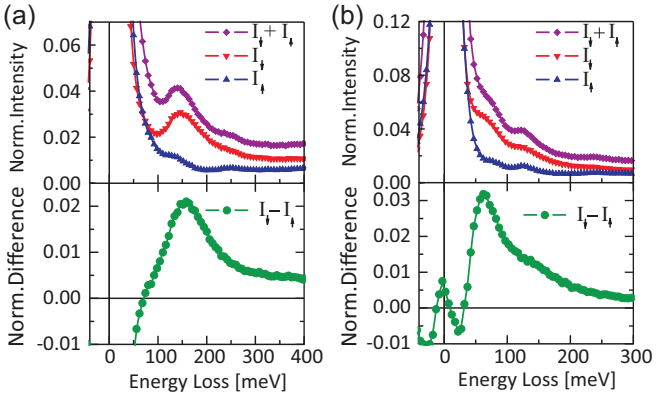


**Fig. 3.** Typical SPEELS spectra recorded at a wave vector of $\vec{q}_{\|} = 0.7(2)$ Å$^1$ on (a) an epitaxial Co(0 0 0 1) film, with a thickness of 8 ML and (b) an epitaxial Fe(1 1 0) film with a thickness of 24 ML grown on W(1 1 0). The spectra are normalized to the total intensity of the quasi-elastic peak. The energy of incident beam was about $E_i = 4$ eV for both cases. The peak in the minority spin channel ($I_\downarrow$) is due to the magnon excitations. The difference spectra ($I_\downarrow - I_\uparrow$) is shown in the lower panels.

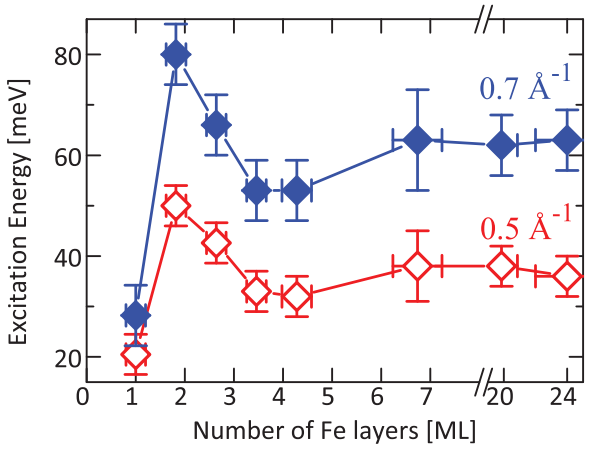


**Fig. 4.** Excitation energy at two different wave vectors (0.5 Å$^{-1}$ and 0.7 Å$^{-1}$) versus the Fe film thickness in Fe(1 1 0)/W(1 1 0) structure [42]. The data of monolayer system are measured at 120 K and all other data are recorded at 300 K.

samples with different thicknesses. The small changes in the geometrical structure influence the electronic structure of the film and thereby changes the effective exchange interaction, which leads to a modification of the magnon energy (dispersion relation). This fact is confirmed by first-principles adiabatic spin dynamics calculations based on density-functional theory (DFT) [42]. Although within this approach the atomic magnetic moments are treated as rigid entities, which precess around the direction of the ferromagnetic ground state (similar to the Heisenberg model), the excitation energies are obtained by means of parameter-free DFT calculations. Within these calculations a mapping of the itinerant electron system onto a Heisenberg Hamiltonian is considered. The calculations performed within the framework of the itinerant electron theory also predicted that the magnon exchange stiffness ($D = E/q^2$, for $q \ll \pi/a$) versus the number of Fe layers shall show a minimum at about 4 ML when the magnons are excited along the $\overline{\Gamma} - \overline{H}$ direction of the surface Brillouin zone [20].

One of the important properties of magnons is the dispersion relation that connects the magnons' energy to their propagation wave vector. Since the main aim of the present paper is to discuss the surface magnons, we mainly discuss the results of magnon excitations in thicker films where the film thickness is large enough and the effects caused by the presence of the film/substrate interfaces are less important. Fig. 5 shows the surface magnon dispersion relation measured on a 24 ML Fe(1 1 0) film grown on W(1 1 0). The first attempt to understand the experimental data would be using the Heisenberg spin Hamiltonian discussed in Section 2. Starting with Eq. 6 and solving it for a system consisting of 24 slabs of Fe in (1 1 0) structure results in 24 modes. The lowest mode is called the acoustic surface mode. The results of such a calculation are given in Fig. 5. For the first approximation we only consider the nearest neighbor coupling ($J_{nn}$) and neglect the next nearest neighbor exchange interaction ($J_{nnn}$). In order to make a comparison to the bulk Fe, the value of $J_{nn}S$ used for this calculation is obtained by fitting the available experimental data of the inelastic neutron scattering experiments measured by Lynn [46]. The fit to the experimental bulk dispersion results in a value of about $J_{nn}S = 13.2$ meV (the fitting curve is shown by the solid red line in Fig. 5(a)). Taking this value and calculating the magnon dispersion relation for a slab consisting of 24 layers of Fe(1 1 0) results in the gray lines, presented in Fig. 5(a). As one can simply recognize from Fig. 5(a) the experimental magnon energies are smaller than the calculated acoustic surface mode of Fe(1 1 0) when the bulk exchange parameter is taken into account. If one tries to adopt the calculated dispersion relation to our experimental dispersion relation [see Fig. 5(b)] a value of about $J_{nn}S = 9.8$ meV will be obtained. This implies that the effective exchange coupling at the surface is smaller than the one of bulk. In the next step one may also consider the next nearest neighbors. Again taking the experimental data of Lynn [46] for bulk dispersion and fitting the data with the next nearest neighbor Heisenberg model will result in $J_{nn}S = 8.9$ meV and $J_{nnn}S = 0.6J_{nn}S$. The results of such an analysis are presented in Fig. 5(c). The red solid curve is the bulk dispersion relation. The gray lines are the results of the Heisenberg model for 24 layers of Fe(1 1 0) in bcc structure, assuming the bulk exchange parameters. Fig. 5(c) indicates that the bulk parameters do not explain the surface magnon

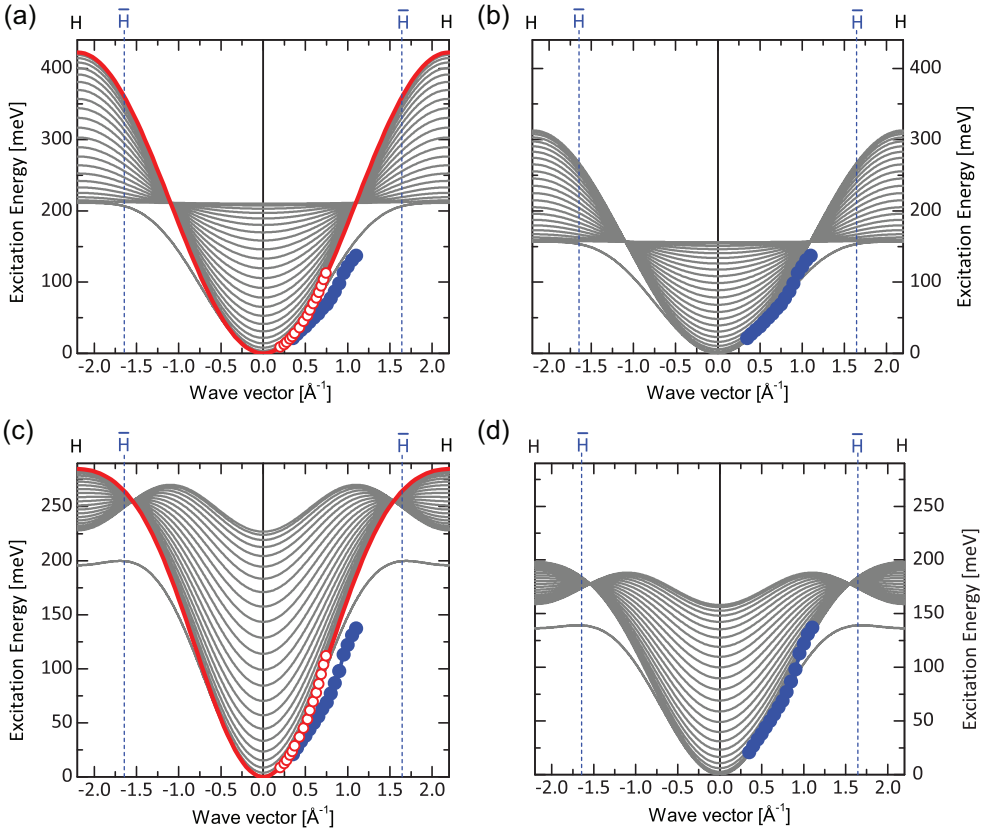


**Fig. 5.** The magnon dispersion relation. The experimental results of surface magnons measured by SPEELS are presented as solid circles. The results of bulk samples measured by inelastic neutron scattering by Lynn [46] are also plotted as open circles for a comparison. (a) The bulk dispersion relation is fitted to a nearest neighbor Heisenberg model (red solid line). The 24 ML film is modeled using the bulk value for $J_{nn}S = 13.2$ meV (gray lines). (b) The nearest neighbor Heisenberg model is adopted to our results of surface magnon dispersion relation resulting in a value of $J_{nn}S = 9.8$ meV. (c) The bulk dispersion relation is fitted to a next nearest neighbor Heisenberg model (red solid line). The 24 ML film is modeled using the bulk values [$J_{nn}S = 8.9$ meV and $J_{nnn}S = 0.6J_{nn}S$ (gray lines)]. (d) The nearest neighbor Heisenberg model is adopted to the surface magnon dispersion relation resulting in values of $J_{nn}S = 6.2$ meV and $J_{nnn}S = 0.6J_{nn}S$. $H$ and $\overline{H}$ denote the bulk and surface Brillouin zone boundaries, respectively. (For interpretation of the references to color in the figure caption and in text, the reader is referred to the web version of the article.)

dispersion relation. A fit to our experimental data reveals that the effective exchange parameters at the surface are smaller than those of the bulk magnons [$J_{nn}S = 6.2$ meV and $J_{nnn}S = 0.6J_{nn}S$, see Fig. 5(d)]. This means that the effective exchange parameter at the surface is smaller than in the bulk. A surface reduction of on-site exchange parameters is expected from a classical Heisenberg Hamiltonian [47,48]. This effect is explained in terms of a reduced coordination of surface atoms. However, ab initio electronic structure calculations has revealed that the interlayer exchange couplings derived from total-energy differences are enhanced at the surfaces over their bulk counterparts [47,48]. Interestingly, in the case of Co(0 0 0 1) films on W(1 1 0) the measured surface magnon dispersion relation could be explained by using the bulk exchange parameter and taking the Heisenberg model [40,41]. In Co it is the nearest neighbor interaction that is important. The second nearest neighbor interaction is very small and can be neglected. It seems that in the case of Co the effective exchange coupling is not very sensitive to the small changes due to the surface effects. Again we would like to emphasize that such a comparison provides just a rough estimation of the effective exchange coupling of the system, since the Heisenberg picture is not an appropriate picture to describe the itinerant electron ferromagnets.

### 4.2. The magnon lifetime

Another important result of our measurements is the estimation of the magnon lifetimes. The broadening of the spectra in energy (frequency) domain can be converted to lifetime. This can be done by a Fourier transformation of the magnon spectra. If one assumes a Lorentzian distribution for the peak in the difference spectra, the magnon lifetime can be simply calculated as following. The Fourier transform of a Lorentzian will be an exponential decay function. The lifetime of a magnon is defined as the time in which the amplitude of the magnon wave packet decays to $e^{-1}$ of its original value at $t = 0$. It is than given by this simple relation:

$$\tau = \frac{2\hbar}{\Delta E}, \tag{9}$$

where $\tau$ is the magnon lifetime and $\Delta E$ represents the intrinsic peak broadening in energy domain. In practice the measured difference spectra might be also affected by the experimental broadening. In order to consider this effect one may consider that the intensity profile is a convolution of a Lorentzian (describing the intrinsic broadening) and a Gaussian (caused by the experimental energy resolution) distribution. We observed in many cases that the experimental broadening has a small influence on the magnons, which have energies above 40 meV (the measured spectra can be fitted by a Lorentzian distribution). The typical values of the magnon lifetime for Fe films measured in our study is within the range of 10–100 fs (for the wave vector range of 1.0–0.4 Å$^{-1}$). As an example, for the data shown in Fig. 3(b) the intrinsic broadening is about $\Delta E \approx 54 \pm 10$ meV, which results in a lifetime of about $\tau = 24 \pm 5$ fs.

## 5. Conclusion

We presented the experimental results of short-wavelength magnon excitations at ferromagnetic surfaces probed by electrons in spin-polarized electron energy-loss spectroscopy. The strong interaction of the electrons with the ferromagnetic surface together with the spin degree of freedom enables one to investigate the surface magnons over the whole energy and momentum range up to the Brillouin zone boundary.

A comparison between Co(0 0 0 1) and Fe(1 1 0) ultrathin films grown on W(1 1 0) shows that in contrast to the case of Co ultrathin films, the magnon energies of Fe films as a function of the film thickness show a minimum at about 4 ML, where the structural relaxation takes place. This observation is attributed to the high sensitivity of the effective exchange interaction of the Fe films to the small changes in the structure.

The surface magnons of Fe(1 1 0) are softer than the one of Fe bulk meaning that the effective exchange parameter at the surface is smaller than the one in the bulk.

The high wave vector magnons possess very short lifetimes being of the order of few tens of femtoseconds. This means that the short-wavelength magnons are strongly confined in time as well as in space.

## Acknowledgements

We acknowledge numerous discussions with the late D.L. Mills the grand pioneer of the theory of spin excitations in itinerant ferromagnets. We also acknowledge discussions with L.M. Sandratskii, A. Ernst, P. Buczek, L. Szunyogh, A.T. Costa and R.B. Muniz. We thank all the present and former co-workers: H. Ibach, R. Vollmer, M. Etzkorn, P.S. Anil Kumar, W.-X. Tang, J. Prokop, I. Tudosa, T.R.F. Peixoto and T.-H. Chuang who have contributed to some experiments discussed here.

## References

[1] S.A. Wolf, D.D. Awschalom, R.A. Buhrman, J.M. Daughton, S. von Molnar, M.L. Roukes, A.Y. Chtchelkanova, D.M. Treger, Science 294 (2001) 1488.
[2] J.A.C. Bland, B. Heinrich, Ultrathin Magnetic Structures. III: Fundamentals of Nanomagnetism, Springer-Verlag, Berlin, Heidelberg, 2005.
[3] A.J. Freeman, Ruqian Wu, J. Magn. Magn. Mater. 100 (1991) 497.
[4] C.A.F. Vaz, J.A.C. Bland, G. Lauhoff, Rep. Prog. Phys. 71 (2008) 056501.
[5] M.N. Baibich, J.M. Broto, A. Fert, F. Nguyen Van Dau, F. Petroff, P. Etienne, G. Creuzet, A. Friederich, J. Chazelas, Phys. Rev. Lett. 61 (1988) 2472.
[6] G. Binasch, P. Grünberg, F. Saurenbach, W. Zinn, Phys. Rev. B 39 (1989) 4828.
[7] B. Heinrich, J.A.C. Bland, Ultrathin Magnetic Structures. IV: Applications of Nanomagnetism, Springer-Verlag, Berlin, Heidelberg, 2005.
[8] J. Fernandez-Rossier, M. Braun, A.S. Núñez, A.H. MacDonald, Phys. Rev. B 69 (2004) 174412.
[9] M. Elsen, O. Boulle, J.-M. George, H. Jaffres, R. Mattana, V. Cros, A. Fert, A. Lemaitre, R. Giraud, G. Faini, Phys. Rev. B 73 (2006) 035303.
[10] B. Hillebrands, K. Ounadiela (Eds.), Topics in Applied Physics, vol. 83, Springer, Berlin, Heidelberg, New York, 2003.
[11] D.L. Mills, S.M. Rezende, Spin Dynamics in Confined Magnetic Structures. II, Springer-Verlag, Berlin, Heidelberg, New York, 2003.
[12] J. Lindner, K. Lenz, E. Kosubek, K. Baberschke, D. Spoddig, R. Meckenstock, J. Pelzl, Z. Frait, D.L. Mills, Phys. Rev. B 68 (2003) 060102.
[13] K. Lenz, H. Wende, W. Kuch, K. Baberschke, K. Nagy, A. Jánossy, Phys. Rev. B 73 (2006) 144424.
[14] Kh. Zakeri, J. Lindner, I. Barsukov, R. Meckenstock, M. Farle, U. von Hörsten, H. Wende, W. Keune, J. Rocker, S.S. Kalarickal, K. Lenz, W. Kuch, K. Baberschke, Z. Frait, Phys. Rev. B 76 (2007) 104416.
[15] K. Baberschke, Phys. Status Solidi B 245 (2008) 174.
[16] I.E. Dzyaloshinskii, Sov. Phys. JETP 5 (1957) 1259.
[17] T. Moriya, Phys. Rev. 120 (1960) 91.
[18] Kh. Zakeri, Y. Zhang, J. Prokop, T.-H. Chuang, N. Sakr, W.-X. Tang, J. Kirschner, Phys. Rev. Lett. 104 (2010) 137203.
[19] R.B. Muniz, D.L. Mills, Phys. Rev. B 66 (2002) 174417.
[20] R.B. Muniz, A.T. Costa, D.L. Mills, J. Phys.: Condens. Matter 15 (2003) S495.
[21] A.T. Costa, R.B. Muniz, D.L. Mills, Phys. Rev. B 68 (2003) 224435.
[22] A.T. Costa, R.B. Muniz, D.L. Mills, Phys. Rev. B 74 (2006) 214403.
[23] R.B. Muniz, A.T. Costa, D.L. Mills, IEEE Trans. Mag. 44 (2008) 1974.
[24] A.T. Costa, R.B. Muniz, J.X. Cao, R.Q. Wu, D.L. Mills, Phys. Rev. B 78 (2008) 054439.
[25] E. Şaşioglu, A. Schindlmayr, C. Friedrich, F. Freimuth, S. Blügel, Phys. Rev. B 81 (2010) 054434.
[26] P. Buczek, A. Ernst, P. Bruno, L.M. Sandratskii, Phys. Rev. Lett. 102 (2009) 247206.
[27] P. Buczek, A. Ernst, L.M. Sandratskii, Phys. Rev. Lett. 105 (2010) 097205.
[28] P. Buczek, A. Ernst, P. Bruno, L.M. Sandratskii, J. Magn. Magn. Mater. 322 (2010) 1396.
[29] P. Buczek, A. Ernst, L.M. Sandratskii, Phys. Rev. Lett. 106 (2011) 157204.
[30] W.X. Tang, Y. Zhang, I. Tudosa, J. Prokop, M. Etzkorn, J. Kirschner, Phys. Rev. Lett. 99 (2007) 087202.
[31] J. Prokop, W.X. Tang, Y. Zhang, I. Tudosa, T.R.F. Peixoto, Kh. Zakeri, J. Kirschner, Phys. Rev. Lett. 102 (2009) 177206.
[32] P. Buczek, A. Ernst, L.M. Sandratskii, Phys. Rev. B 84 (2011) 174418.
[33] H. Ibach, D. Bruchmann, R. Vollmer, M. Etzkorn, P.S. Anil Kumar, J. Kirschner, Rev. Sci. Instrum. 74 (2003) 4089.

[34] Kh. Zakeri, J. Kirschner, Probing Magnons by Spin-Polarized Electrons, in: S.O. Demokritov, A.N. Slavin (Eds.), Topics in Applied Physics, Magnonics, Springer-Verlag, Berlin, Heidelberg, 2012, http://dx.doi.org/10.1007/978-3-642-30247-3_7.
[35] J. Kessler, Polarized Electrons, Springer-Verlag, Berlin, Heidelberg, New York, Tokyo, 1985.
[36] J. Kirschner, Phys. Rev. Lett. 55 (1985) 973.
[37] J. Kirschner, Springer Tracts in Modem Physics, vol. 106, Springer, Heidelberg, 1985.
[38] J. Kirschner, in: R. Feder (Ed.), Polarized Electrons in Surface Physics, World Scientific, Singapore, 1985.
[39] Y. Zhang, P.A. Ignatiev, J. Prokop, I. Tudosa, T.R.F. Peixoto, W.X. Tang, Kh. Zakeri, V.S. Stepanyuk, J. Kirschner, Phys. Rev. Lett. 106 (2011) 127201.
[40] M. Etzkorn, P.S. Anil Kumar, W. Tang, Y. Zhang, J. Kirschner, Phys. Rev. B 72 (2005) 184420.
[41] M. Etzkorn, P.S. Anil Kumar, J. Kirschner, in: H. Kronmüller, S. Parkin (Eds.), Handbook of Magnetism and Advanced Magnetic Materials, vol. 3: Novel Techniques for Characterizing and Preparing Samples, Wiley & Sons, Ltd., 2007.
[42] Y. Zhang, P. Buczek, L.M. Sandratskii, W.X. Tang, J. Prokop, I. Tudosa, T.R.F. Peixoto, Kh. Zakeri, J. Kirschner, Phys. Rev. B 81 (2010) 094438.
[43] D. Sander, R. Skomski, C. Schmidthals, A. Enders, J. Kirschner, Phys. Rev. Lett. 77 (1996) 2566.
[44] D. Sander, A. Enders, C. Schmidhals, D. Reuter, J. Kirschner, Surf. Sci. 402–404 (1998) 351.
[45] H.J. Elmers, Int. J. Mod. Phys. B 9 (1995) 3115.
[46] J.W. Lynn, Phys. Rev. B 11 (1974) 2624.
[47] I. Turek, S. Blügel, G. Bihlmayer, P. Weinberger, Czech. J. Phys. 53 (2003) 81.
[48] I. Turek, J. Kudrnovsky, V. Drchal, P. Bruno, Philos. Mag. 86 (2006) 1713.